

Investigation of New Coordination Modes for Coordinatively Unsaturated (Dithiolato)cobalt(III) Complex $[(\eta^5\text{-Cp})\text{Co}(1,2\text{-S}_2\text{C}_2\text{B}_{10}\text{H}_{10}\text{-S,S})]$

Jae-Hong Won,[†] Dae-Hyun Kim,[†] Bo Young Kim,[‡] Sung-Joon Kim,[†] Chongmok Lee,^{*,‡} Sungil Cho,[§] Jaejung Ko,^{*,†} and Sang Ook Kang^{*,†}

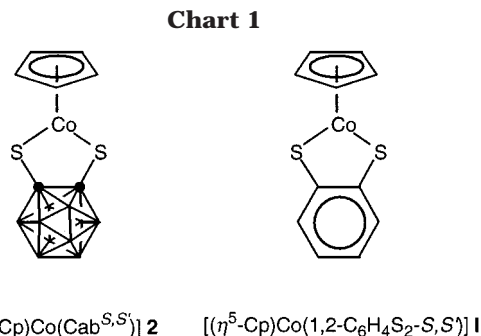
Department of Chemistry, Korea University, 208 Seochang, Chochiwon, Chung-nam 339-700, Korea, Department of Chemistry, Ewha Womans University, Seoul 120-750, Korea, and Department of Chemical Engineering, Junnong-dong 90, Seoul City University, Seoul 130-743, Korea

Received October 12, 2001

A mononuclear 16-electron Cp-cobalt(III)-dithiolate complex of the general formula $[(\eta^5\text{-Cp})\text{Co}(\text{Cab}^{\text{S,S}})]$ (**2**) ($\text{Cab}^{\text{S,S}} = 1,2\text{-S}_2\text{C}_2\text{B}_{10}\text{H}_{10}\text{-S,S}$) has been prepared by treatment of $\text{CpCo}(\text{CO})\text{I}_2$ with the corresponding dilithium dithiolato ligand $\text{Li}_2\text{Cab}^{\text{S,S}}$ (**1**). Experiments aimed at the characterization of new coordination modes for **2** are described. The reaction of **2** with $\text{BH}_3\cdot\text{THF}$ produces an unexpected bimetallic cobalt dithiolate complex, $[(\eta^5\text{-Cp})\text{Co}]_2(\text{Cab}^{\text{S,S}})]$ (**3**). A second new bonding mode for **2** was generated by treatment of **2** with Lewis bases (L) to give $[(\eta^5\text{-Cp})\text{Co}(\text{Cab}^{\text{S,S}})(\text{L})]$ (L = CNBu^t (**4a**), PETe_3 (**4b**)), the 18-electron species of which consists of a mononuclear **2** coordinated through a dative Co-L bond. A third new bonding mode for **2** is illustrated by $[(\eta^5\text{-Cp})\text{Co}(\text{Cab}^{\text{S,S}})(\eta^1\text{-CH}_2\text{SiMe}_3\text{-S})]$ (**5**). Reaction of **2** with (trimethylsilyl)diazomethane resulted in the formation of the alkylidene-bridged complex **5**, containing a Co-C-S three-membered ring. The formation of **4** and **5** has also been investigated electrochemically. Consequently, the addition of organic and organometallic compounds into the Co-S bond of **2** has been investigated. Thus, the syntheses of half-sandwich cobalt(III) complexes $[(\eta^5\text{-Cp})\text{Co}(\text{Cab}^{\text{S,S}})(\text{L})]$ [L = $\eta^5\text{-CpCo-S,S}$ (**3**), $\eta^1\text{-R}_1\text{C}=\text{CR}_2\text{-S}$ (**6**: $\text{R}_1 = \text{R}_2 = \text{COOMe}$ (**6a**); $\text{R}_1 = \text{H}$ $\text{R}_2 = \text{Ph}$ (**6b**); $\text{R}_1 = \text{H}$ $\text{R}_2 = \text{SiMe}_3$ (**6c**))] are reported. In addition, the solid-state structures of **3**, **4b**, **5**, and **6a** were characterized by single-crystal X-ray analyses.

Introduction

The synthesis and study of organometallic complexes possessing an ancillary *o*-carboranyl dithiolato ligand have continued to receive attention.¹ To further develop the chemistry of *o*-carboranyl dithiolate and assess its ability to form reactive transition-metal complexes, we have examined its reactions with a selection of cyclopentadienyl transition-metal complexes. In particular, we have been interested in obtaining coordinatively unsaturated low-valent metal complexes, capable of binding biologically interesting substrates such as acetylene, CO, diazenes, or dinitrogen. It was therefore of interest to investigate the possibility of synthesizing such coordinatively unsaturated low-valent metal complexes bearing both bulky *o*-carborane² and cyclopentadienyl units that might potentially stabilize the 16-electron metal center,³ as shown in Chart 1.



Our interest in the synthesis and reactivity of coordinatively unsaturated low-valent metal complexes⁴ now leads us to explore the use of an *o*-carboranyldithiolato ligand in the formation of metalladithiolene ring complexes.⁵ An attractive feature of such reactive metalladithiolene ring complexes is the unsaturation at the

[†] Korea University.

[‡] Ewha Womans University.

[§] Seoul City University.

(1) (a) Base, K.; Grinstaff, M. W. *Inorg. Chem.* **1998**, *37*, 1432. (b) Crespo, O.; Gimeno, M. C.; Jones, P. G.; Laguna, A. *J. Chem. Soc., Dalton Trans.* **1997**, 1099. (c) Crespo, O.; Gimeno, M. C.; Jones, P. G.; Laguna, A. *J. Chem. Soc., Chem. Commun.* **1993**, 1696. (d) Contreras, J. G.; Silva-trivino, L. M.; Solis, M. E. *J. Coord. Chem.* **1986**, *14*, 309. (e) Smith, H. D., Jr.; Robinson, M. A.; Papetti, S. *Inorg. Chem.* **1967**, *6*, 1014. (f) Smith, H. D., Jr.; Obenland, C. O.; Papetti, S. *Inorg. Chem.* **1966**, *5*, 1013. (g) Smith, H. D., Jr. *J. Am. Chem. Soc.* **1965**, *87*, 1817.

(2) Beall, H. In *Boron Hydride Chemistry*; Muetterties, E., Ed.; Academic Press: New York, 1975; Chapter 9.

(3) (a) Mashima, K.; Kaneyoshi, H.; Kaneko, S.; Mikami, A.; Tani, K.; Nakamura, A. *Organometallics* **1997**, *16*, 1016. (b) Michelman, R. I.; Ball, G. E.; Bergman, R. G.; Anderson, R. A. *Organometallics* **1994**, *13*, 869. (c) Garcia, J. J.; Torrens, H.; Adames, H.; Bailey, N. A.; Scacklady, A.; Matlis, P. M. *J. Chem. Soc., Dalton Trans.* **1993**, 1529. (d) Michelman, R. I.; Anderson, R. A.; Bergman, R. G. *J. Am. Chem. Soc.* **1991**, *113*, 5100. (e) Garcia, J. J.; Torrens, H.; Adams, H.; Bailey, N. A.; Matlis, P. M. *J. Chem. Soc., Chem. Commun.* **1991**, 74. (f) Klein, D. P.; Kloster, G. M.; Bergman, R. G. *J. Am. Chem. Soc.* **1990**, *112*, 2022.

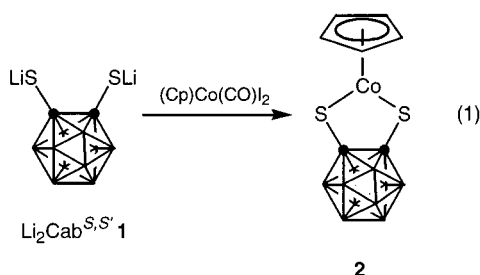
(4) Ko, J.; Kang, S. O. *Adv. Organomet. Chem.* **2001**, *47*, 61.

metal and sulfur atoms.⁶ It has been observed that addition reactions between the metal and sulfur atoms are reactions characteristic of the metalladithiolene ring complex $[(\eta^5\text{-Cp})\text{Co}(1,2\text{-C}_6\text{H}_4\text{S}_2\text{-S,S})]$ (**1**).

Taking into account the work of A. Sugimori⁷ and other workers,⁸ we recently prepared $[(\eta^5\text{-Cp})\text{Co}(\text{Cab}^{\text{S,S}})]$ (**2**) by salt metathesis using *o*-carboranyl dithiolato ligand $\text{Li}_2\text{Cab}^{\text{S,S}}$ (**1**). This species is therefore a promising starting point for the exploration of new *o*-carboranyl-based metalladithiolene ring complexes. Through such efforts, we have discovered three new bonding modes of the *o*-carboranyl dithiolato ligand.

Results and Discussion

Synthesis of Coordinatively Unsaturated Metal Complex. The reaction of $[(\text{Cp})\text{Co}(\text{CO})\text{I}_2]$ (3 mmol) with the dilithium salt $\text{Li}_2\text{Cab}^{\text{S,S}}$ (**1**) (3.2 equiv) in THF afforded an 83% yield of **2** as an air-stable red solid (eq 1).

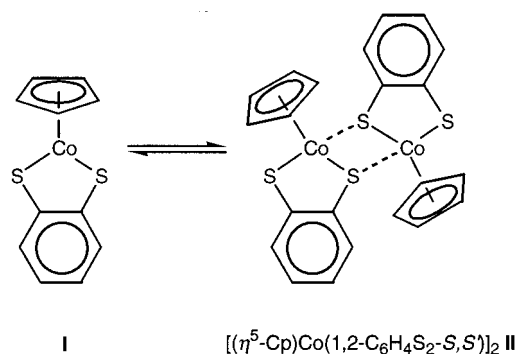


Thus, analytical and spectroscopic data support the formulation of **2** as a mononuclear 16-electron *o*-carboranyl dithiolato cobalt(III) complex. Such a monomeric 16-electron thiolato cobalt(III) structure has been reported for the benzenedithiolate complex $[(\text{Cp})\text{Co}(1,2\text{-C}_6\text{H}_4\text{S}_2\text{-S,S})]$ (**1**).⁹ A reversible mononuclear–dinuclear interconversion^{10–12} in the benzenedithiolate complexes was also reported by Miller et al. for **1** as shown in Chart 2.

On the contrary, we have isolated the mononuclear cobalt(III) analogue **2** and have found that it exists only in the monomeric form. Formation of a dimeric species in solution was not observed.

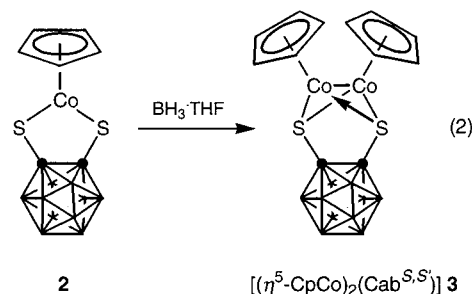
Formation of Bimetallic Cobalt Complex $[(\eta^5\text{-Cp})\text{Co}]_2(\text{Cab}^{\text{S,S}})$ (3**).** The cyclic voltammogram (CV) of complex **2** in CH_2Cl_2 is shown in Figure 1A and consists of two major redox responses, i.e., a reversible 0/–1

Chart 2



reduction wave of the central metal atom ($\text{Co}^{3+}|\text{Co}^{2+}$) at $E_{1/2} = -0.59$ V and an irreversible +1/0 oxidation wave of the cobaltadithiolene ring at $E_{\text{pa}} = 0.98$ V. A closer examination reveals the presence of another redox process at the less positive potential of +0.17 V, which implies the presence of another electroactive species. It is assumed to be the dinuclear complex **3**, because complex **3** is a stable 18-electron species.

To better understand the electrochemical results, we undertook the preparative-scale synthesis of **3**. Surprisingly, treatment of a solution of **2**, which is red, with 5 equiv of $\text{BH}_3\cdot\text{THF}$ gave a green solution, from which we isolated the green solid **3** (eq 2).



The ¹H NMR spectrum of **3** consists of a single sharp signal in the Cp region, consistent with a symmetric structure and a diamagnetic ground state. X-ray crystallographic (vide infra) and elemental analyses showed that the product is an unprecedented bimetallic species, $[(\eta^5\text{-Cp})\text{Co}]_2(\text{Cab}^{\text{S,S}})$ (**3**), in which each cobalt center is connected with a dithiolato ligand. The asymmetric unit contains five independent molecules with almost identical structures, one of which is shown in Figure 2. Selected bond distances and angles are summarized in Tables 2 and 3. In the solid state, **3** consists of a symmetrically coordinated bimetallic complex as shown in Figure 2. The two halves of the $(\eta^5\text{-Cp})\text{Co}$ units are linked through a pair of Co–S and Co–Co bonds such that each cobalt atom is three-coordinate with a cobaltadithiolene ring. The diamagnetic nature of **3** indicates the presence of a $\text{Co}^{3+}\text{–Co}^{3+}$ single bond. The intramolecular distance between the two Co atoms is 2.369(2) (av) Å, indicating the presence of a metal–metal bond interaction.

The cyclic voltammogram of complex **3** was measured in CH_2Cl_2 , which showed two successive oxidation waves, as shown in Figure 1B. Interestingly, the CV of **3** shows no reduction wave corresponding to a 0/–1 redox couple, but a reversible oxidation wave at $E_{1/2}$ of 0.19 V with $\Delta E_p = 73$ mV, and further irreversible

(5) (a) Bae, J.-Y.; Lee, Y.-J.; Kim, S.-J.; Ko, J.; Cho, S.; Kang, S. O. *Organometallics* **2000**, *19*, 1514. (b) Kim, D.-H.; Ko, J.; Park, K.; Cho, S.; Kang, S. O. *Organometallics* **1999**, *18*, 2738. (c) Bae, J.-Y.; Park, Y.-L.; Ko, J.; Park, K.-I.; Cho, S.-I.; Kang, S. O. *Inorg. Chim. Acta* **1999**, *289*, 141.

(6) Sellmann, D.; Geck, M.; Knoch, F.; Ritter, G.; Dengler, J. *J. Am. Chem. Soc.* **1991**, *113*, 3819.

(7) Sugimori, A.; Akiyama, T.; Kajitani, M.; Sugiyama, T. *Bull. Chem. Soc. Jpn.* **1999**, *72*, 879.

(8) (a) Fourmigué, M. *Coord. Chem. Rev.* **1998**, *178–180*, 823. (b) Fourmigué, M.; Domercq, B.; Jourdain, I. V.; Molinié, P.; Guyon, F.; Amaudrut, J. *Chem. Eur. J.* **1998**, *4*, 1714. (c) Jourdain, I. V.; Fourmigué, M.; Guyon, F.; Amaudrut, J. *J. Chem. Soc., Dalton Trans.* **1998**, 483. (d) Jourdain, I. V.; Fourmigué, M.; Guyon, F.; Amaudrut, J. *Organometallics* **1999**, *18*, 1834.

(9) Heck, R. F. *Inorg. Chem.* **1968**, *7*, 1513.

(10) Miller, E. J.; Brill, T. B.; Rheingold, A. L.; Fultz, W. C. *J. Am. Chem. Soc.* **1983**, *105*, 7580.

(11) Nozawa, S.; Sugiyama, T.; Kajitani, M.; Akiyama, T.; Sugimori, A. *Chem. Lett.* **1996**, 191.

(12) Xi, R.; Abe, M.; Suzuki, T.; Nishioka, T.; Isobe, K. *J. Organomet. Chem.* **1997**, *549*, 117.

Table 1. X-ray Crystallographic Data and Processing Parameters for Compounds **3**, **4b**, **5**, and **6**

	3	4b	5	6
formula	C ₁₂ H ₂₀ B ₁₀ S ₂ Co ₂	C ₁₃ H ₃₀ B ₁₀ CoPS ₂	C ₁₁ H ₂₅ B ₁₀ SiS ₂ Co	C ₁₃ H ₂₁ B ₁₀ O ₄ S ₂ Co
fw	454.36	448.49	416.55	472.45
cryst class	triclinic	monoclinic	triclinic	triclinic
space group	<i>P</i> 1	<i>C</i> 2/ <i>c</i>	<i>P</i> 1	<i>P</i> 1
<i>Z</i>	10	8	2	2
cell constants				
<i>a</i> , Å	12.056(4)	27.045(1)	7.8599(4)	10.0447(7)
<i>b</i> , Å	15.412(2)	11.382(1)	9.7306(8)	11.5109(6)
<i>c</i> , Å	28.86(1)	15.002(1)	14.7510(7)	12.0399(5)
<i>V</i> , Å ³	4841(2)	4415.2(5)	1048.2(1)	1099.8(1)
α , deg	101.24(2)		102.517(5)	115.980(3)
β , deg	96.72(3)	107.05(2)	104.820(4)	106.281(5)
γ , deg	110.06(2)		96.329(5)	102.960(5)
μ , mm ⁻¹	1.921	1.036	1.067	0.988
cryst size, mm	0.1 × 0.2 × 0.2	0.3 × 0.3 × 0.6	0.2 × 0.2 × 0.3	0.15 × 0.2 × 0.3
<i>D</i> _{calcd} , g/cm ³	1.558	1.349	1.320	1.427
<i>F</i> (000)	2280	1856	428	480
radiation		Mo K α (λ = 7170 Å)		
θ range, deg	1.45–25.97	1.58–25.98	1.48–25.97	2.04–25.97
<i>h</i> , <i>k</i> , <i>l</i> collected	+14, \pm 19, \pm 35	\pm 33, +14, +18	+9, \pm 11, \pm 18	+12, \pm 14, \pm 14
no. of reflns collected/unique	19819/18835	8680/4326	3969/3679	4624/4325
no. of data/restraints/params	18835/0/1271	4326/0/262	3679/0/244	4325/0/288
goodness-of-fit on <i>F</i> ²	1.853	0.884	0.835	0.877
final <i>R</i> indices [<i>I</i> > 2 σ (<i>I</i>)]	^a <i>R</i> 1 = 0.0966, ^b <i>wR</i> 2 = 0.2750	^a <i>R</i> 1 = 0.0310, ^b <i>wR</i> 2 = 0.0925	^a <i>R</i> 1 = 0.0364, ^b <i>wR</i> 2 = 0.1019	^a <i>R</i> 1 = 0.0480, ^b <i>wR</i> 2 = 0.1250
<i>R</i> indices (all data)	^a <i>R</i> 1 = 0.1563, ^b <i>wR</i> 2 = 0.2994	^a <i>R</i> 1 = 0.0419, ^b <i>wR</i> 2 = 0.1033	^a <i>R</i> 1 = 0.0771, ^b <i>wR</i> 2 = 0.1249	^a <i>R</i> 1 = 0.1329, ^b <i>wR</i> 2 = 0.1571
largest diff peak and hole, e/Å ³	1.903 and -0.652	0.408 and -0.722	0.352 and -0.264	0.298 and -0.337

^a *R*₁ = $\sum ||F_o| - |F_c||$ (based on reflections with $F_o^2 > 2\sigma(F_o^2)$). ^b *wR*₂ = $[\sum [w(F_o^2 - F_c^2)^2] / \sum [w(F_o^2)^2]]^{1/2}$; $w = 1/[\sigma^2(F_o^2) + (0.095P)^2]$; $P = [\max(F_o^2, 0) + 2F_c^2]/3$ (also with $F_o^2 > 2\sigma(F_o^2)$).

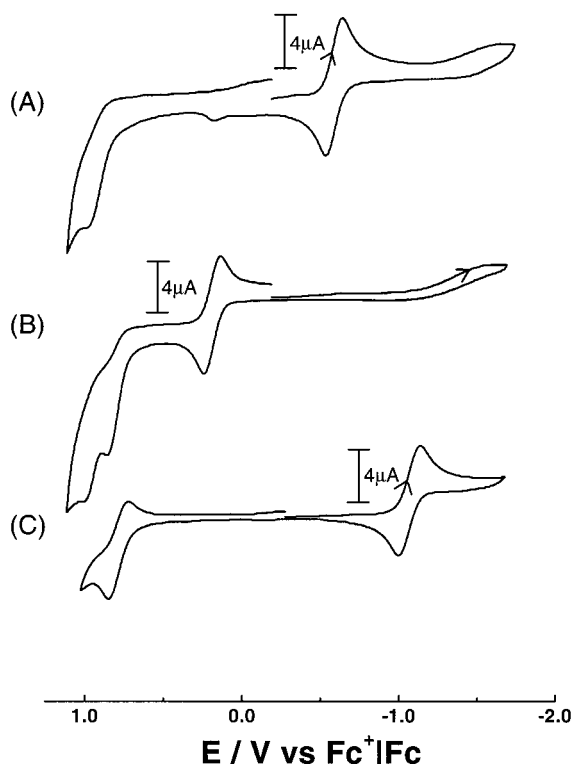


Figure 1. Cyclic voltammograms of 1 mM [(η^5 -Cp)Co-(Cab^{5,5})] (**2**) (A), [(η^5 -Cp)Co)₂(Cab^{5,5})] (**3**) (B), and [(η^5 -Cp*)Co(Cab^{5,5})] (**III**) (C) at a platinum disk electrode with negative initial scan direction; in CH₂Cl₂ containing 0.1 M TBAB; ν = 0.1 V s⁻¹.

oxidation waves at E_{pa} of 0.86 and 1.00 V are seen (Figure 1B). Thus, the reversible oxidation wave at $E_{1/2}$ = 0.19 V is assignable to the oxidation of the bimetallic Co–Co bond by removal of an electron, whereas the other two consecutive irreversible oxidation processes

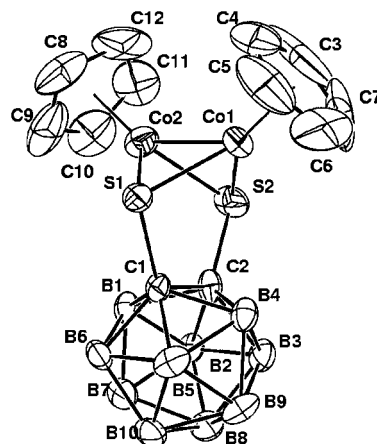


Figure 2. Molecular structure of **3** with atom labeling; ellipsoids show 30% probability levels, and hydrogen atoms have been omitted for clarity.

at E_{pa} of 0.86 and 1.00 V result from the oxidation of the dithiolene sulfur atoms. An analogous electron-transfer series including a bimetallic species with Ru³⁺–Ru³⁺ metal centers has been observed for the oxidation of Cp*Ru(μ -SPh)₃RuCp*.¹³

The reaction of **2** with BH₃·THF deserves a special comment. In this case, careful control of the reaction conditions (–78 °C, 3 h) was necessary to prevent the formation of byproducts such as polynuclear metal complexes. Working at room temperature, however, we always obtained complex mixtures of compounds containing large amounts of polynuclear metal complexes. The ¹¹B NMR spectrum of the inorganic residue remaining after the reaction by BH₃·THF indicates that a high proportion of the boron remains bound to the cobalt center and retains the metallaborane structure as

(13) Dev. S.; Mizobe, Y.; Hiday, M. *Inorg. Chem.* **1990**, *29*, 4797.

Table 2. Selected Interatomic Distances (Å) in 3, 4b, 5, and 6a

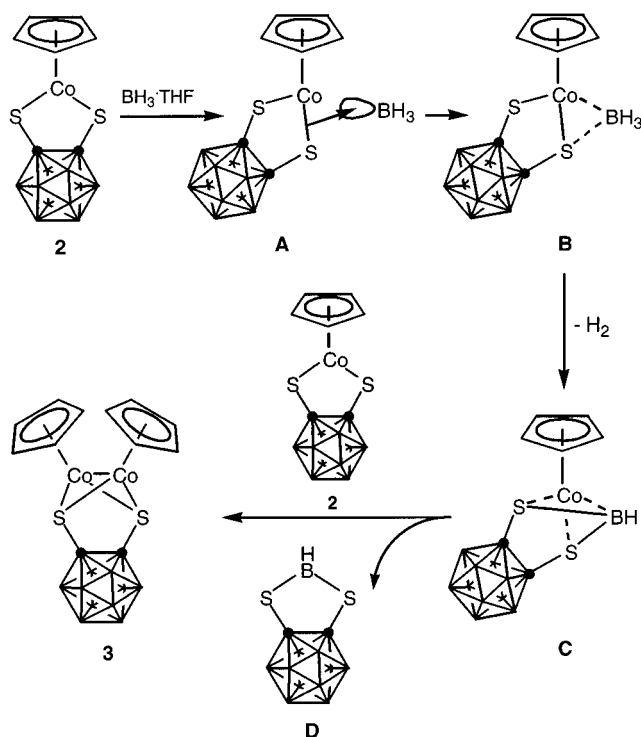
Compound 3					
Co(1)–Co(2)	2.369(2)	Co(1)–S(1)	2.211(2)	Co(1)–S(2)	2.222(3)
Co(2)–S(1)	2.197(2)	Co(2)–S(2)	2.205(3)		
Compound 4b					
Co(1)–S(1)	2.2548(5)	Co(1)–S(2)	2.2609(6)	S(1)–C(1)	1.7816(2)
S(2)–C(2)	1.787(2)	Co(1)–P(1)	2.2123(5)		
Compound 5					
Co(1)–S(1)	2.265(1)	Co(1)–S(2)	2.157(1)	Co(1)–C(8)	1.994(4)
S(2)–C(8)	1.759(3)	S(1)–C(1)	1.772(4)	S(2)–C(2)	1.810(3)
Compound 6a					
Co(1)–S(1)	2.247(2)	Co(1)–S(2)	2.246(1)	Co(1)–C(11)	1.912(5)
S(2)–C(10)	1.777(5)	C(10)–C(11)	1.340(7)	S(1)–C(1)	1.778(5)
S(2)–C(2)	1.794(5)				

Table 3. Selected Interatomic Angles (deg) in 3, 4b, 5, and 6a

Compound 3					
S(1)–Co(1)–S(2)	84.72(9)	S(1)–Co(2)–S(2)	85.46(9)	Co(1)–S(1)–Co(2)	65.03(8)
Co(1)–S(2)–Co(2)	64.72(8)				
Compound 4b					
P(1)–Co(1)–S(1)	91.82(2)	P(1)–Co(1)–S(2)	93.15(2)	S(1)–Co(1)–S(2)	91.59(2)
C(1)–S(1)–Co(1)	103.43(6)	C(2)–S(2)–Co(1)	103.43(6)		
Compound 5					
S(1)–Co(1)–S(2)	94.74(4)	S(1)–Co(1)–C(8)	91.8(1)	S(2)–Co(1)–C(8)	50.0(1)
Co(1)–S(2)–C(8)	60.2(1)	S(2)–C(8)–Co(1)	69.9(1)	C(1)–S(1)–Co(1)	102.7(1)
C(2)–S(2)–Co(1)	105.2(1)				
Compound 6a					
S(1)–Co(1)–S(2)	93.51(5)	S(2)–Co(1)–C(11)	72.4(2)	S(1)–Co(1)–C(11)	92.8(1)
C(1)–S(1)–Co(1)	103.8(2)	C(2)–S(2)–Co(1)	105.7(2)	Co(1)–S(2)–C(10)	79.3(2)
S(2)–C(10)–C(11)	104.0(4)	C(10)–C(11)–Co(1)	104.4(4)		

deduced from the chemical shift and coupling constant. Thus, as expected, only the bimetallic complex **3** was obtained in moderate yield (47%) working at low temperature ($-78\text{ }^{\circ}\text{C}$). This pathway suggests a pronounced basicity of mononuclear dithiolato complex **2** imposed by the dithiolato moiety, which initiates its transformation to the corresponding bimetallic complex **3**.

Therefore, the formation of bimetallic complex **3** may be explained by a series of steps, as shown in Scheme 1. A reasonable reaction sequence for the formation of **3** (Scheme 1) involves the initial insertion of the BH_3 group into one of the Co–S bonds, leading to three-membered intermediate **B**, followed by another insertion of the coordinated BH_3 group into the remaining Co–S bond and concomitant loss of H_2 . It had been well-established that metalladitholene rings underwent addition reactions to the metal and sulfur atoms due to their unsaturation.⁶ The cyclization product **D** then is formed in a reductive elimination process with the extrusion of a CpCo fragment. Successive migration of the CpCo unit to the other dithiolene ring in our case then would afford the bimetallic species **3**. Such a formation of a cobaltaborane intermediate **C** is further supported by the isolation of dithiolatoborane complex **D**. In fact, a five-membered dithiolatoborane was isolated as white powders in 30% yield. The identity of compound **D** was confirmed by its IR, ^{11}B , and mass spectrum. These spectral data were identical to those Smith¹⁴ had observed for compound **D**. In particular, the IR spectrum shows the normal B–H stretching and deformation modes of the σ -carboranyl B–H unit at 2600 and 730 cm^{-1} , the expected B–H stretch of the single exo-cyclic B–H at 2495 cm^{-1} , and a strong

Scheme 1. Possible Reaction Sequence for the Formation of 3

absorption near 795 cm^{-1} , characteristic of the heterocyclic dithiolate five-membered ring.¹⁵ We emphasize that these suggested reaction courses have no further experimental support and are entirely speculative.

(15) (a) Smith, H. D., Jr.; Robinson, M. A.; Papetti, S. *Inorg. Chem.* **1967**, *6*, 1014. (b) Smith, H. D., Jr.; Obenland, C. O.; Papetti, S. *Inorg. Chem.* **1966**, *5*, 1013.

(14) Smith, H. D., Jr.; Hohnstedt, L. F. *Inorg. Chem.* **1968**, *7*, 1061.

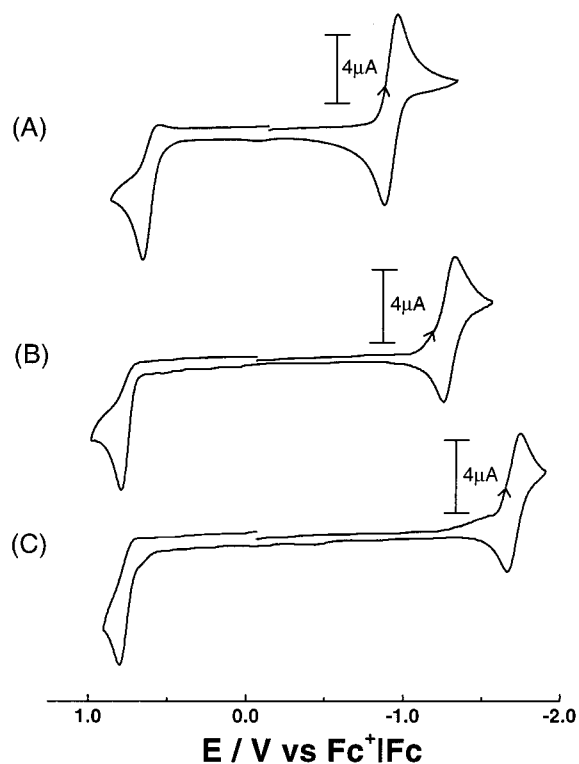


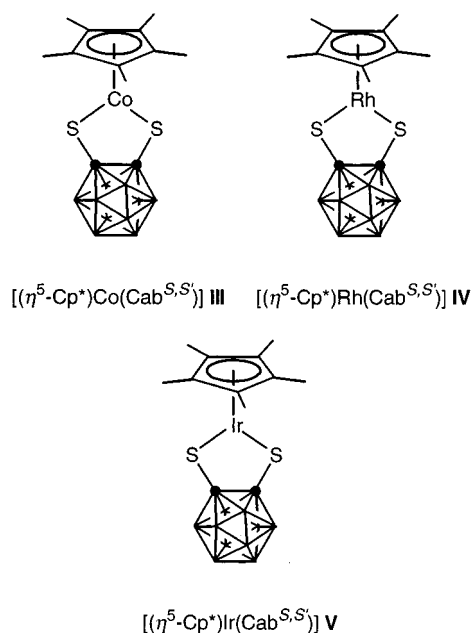
Figure 3. Cyclic voltammograms of 1 mM $[(\eta^5\text{-Cp}^*)\text{Co}(\text{Cab}^{S,S})]$ (**III**) (A), $[(\eta^5\text{-Cp}^*)\text{Rh}(\text{Cab}^{S,S})]$ (**IV**) (B), and $[(\eta^5\text{-Cp}^*)\text{Ir}(\text{Cab}^{S,S})]$ (**V**) (C) at a platinum disk electrode with negative initial scan direction; in CH_3CN containing 0.1 M TBAP; $\nu = 0.1 \text{ V s}^{-1}$.

Effect of Bulky Ancillary Cp* Unit. The cobalt complex **2** exhibits small irreversible oxidation waves at the potential of +0.17 V. These oxidation peaks are ascribed to the formation of bimetallic species. However, in the oxidation of the complex $[(\eta^5\text{-Cp}^*)\text{Co}(\text{Cab}^{S,S})]$ (**III**) (Figure 1C), an electrochemical silence exists between 0/−1 reduction and +1/0 oxidation at the first cycle of CVs, which implies the absence of another reduction product. The formation of bimetallic species is further tested by the chemical reaction using $\text{BH}_3\cdot\text{THF}$. Whereas the metalladithiolene complex **2** undergoes BH_3 addition reactions at the metal and sulfur to form bimetallic complex **3**, the Cp* complex **III** fails to undergo bimetalation processes.

Thus, a rationale with respect to bimetalation for the BH_3 addition reactions, based on the steric bulkiness of the ancillary Cp* ligand, has been established. Using cobalt metal complexes of a different nature of the ancillary ligand (Cp vs Cp*), it has been possible for us to show that bulkiness of the ancillary Cp* ligand in the metal complexes plays an important role in the bimetalation process. Increasing bulkiness of the pentamethylcyclopentadienyl ligand in **III** hampers the formation of bimetallic complexes as found in **3** and instead favors the formation of mononuclear complexes.

Effect of the Metals: $[(\eta^5\text{-Cp}^*)\text{M}(\text{Cab}^{S,S})]$ ($\text{M} = \text{Co}$ (**III**); Rh (**IV**); Ir (**V**)). Typical cyclic voltammograms of the rhodium and iridium complexes, together with that of the cobalt complex, are shown in Figure 3. Thus, Figure 3A–C displays CVs of $[(\eta^5\text{-Cp}^*)\text{Co}(\text{Cab}^{S,S})]$ (**III**), $[(\eta^5\text{-Cp}^*)\text{Rh}(\text{Cab}^{S,S})]$ (**IV**), and $[(\eta^5\text{-Cp}^*)\text{Ir}(\text{Cab}^{S,S})]$ (**V**), respectively, taken in CH_3CN containing 0.1 M TBAP at a scan rate (ν) of 0.1 V s^{-1} . Each of the CVs of **III**,

Chart 3



IV, and **V** shows two major redox responses, i.e., a reversible 0/−1 reduction wave of the central metal atom ($\text{M}^{3+}|\text{M}^{2+}$)¹ at $E_{1/2} = -0.92$, -1.30 , and -1.67 V and an irreversible +1/0 oxidation wave of the metalladithiolene ring at $E_{\text{pa}} = 0.65$, 0.79 , and 0.87 V , respectively. The complexes **III**, **IV**, and **V** exhibit well-defined reversible one-electron reduction waves similarly to the case of the cobalt complex **2**. This redox pattern illustrates the similarity in electronic configurations among **III**, **IV**, and **V**, as shown in Chart 3.

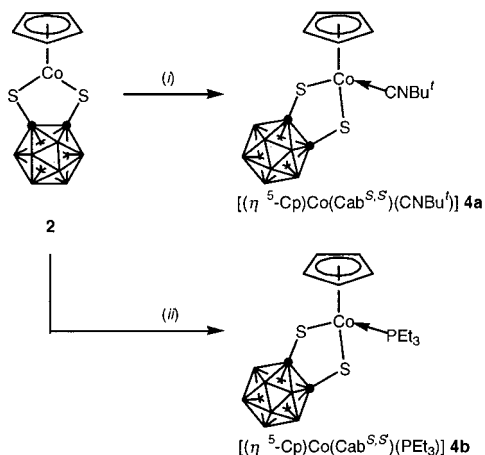
The reduction of Cp or Cp* metalladithiolene complexes occurs at the metal site. The sequence of redox potentials of the cathodic wave which is reversible in all cases can be rationalized in the following way: the degree of difficulty to be reduced is in the order of the iridium > rhodium > cobalt complex due to the lower electronegativity. The oxidation of the metalladithiolene complexes is irreversible. The gaps between the reduction and oxidation potentials in the rhodium and iridium complexes are larger than those of the cobalt complex. These results agreed with those of $[(\text{Cp})\text{M}(\text{cod})]$ ($\text{cod} = 1,5\text{-cyclooctadiene}$)¹⁶ and $[(\text{Cp})\text{M}(\text{CO})_2]$ ($\text{M} = \text{Co}$ and Rh).¹⁷

The shift of E_{pa} from Co to Rh and Ir for oxidation is less than one-third of that for reduction. This small shift in the oxidation potential would indicate that the oxidation occurs at the sulfur atoms, which are less affected by metal atoms.

Synthesis and Characterization of Complexes $[(\eta^5\text{-Cp})\text{Co}(\text{Cab}^{S,S})(\text{L})]$ ($\text{L} = \text{CNBu}^t$ (4a**), PEt_3 (**4b**), CO (**4c**)).** As already reported for analogous complex **V**,^{5c} the 16-electron complex **2** acts as a Lewis acid and forms 1:1 adducts with *tert*-butyl isocyanide and triethylphosphine. Our results are closely related to those of the reported 16-electron iridium and rhodium complexes such as $[(\eta^5\text{-Cp}^*)\text{Ir}(\text{Cab}^{S,S})(\text{L})]$ ($\text{L} = \text{CNBu}^t$, PMe_3 , CO)^{5c} and $[(\eta^5\text{-Cp}^*)\text{Rh}(\text{Cab}^{S,S})(\text{PMe}_3)]$.¹⁸ The new complexes

(16) Connelly, N. G.; Geiger, W. E.; Lane, G. A.; Raven, S. J.; Rieger, P. H. *J. Am. Chem. Soc.* **1986**, *108*, 6219.

(17) Lichtenberger, D. L.; Calabro, D. C.; Kellogg, G. E. *Organometallics* **1984**, *3*, 1623.

Scheme 2. Addition Reaction of 16-Electron Metal Complexes of **2^a**


^a Legend: (i) CNBu^t, toluene, 25 °C; (ii) PEt₃, toluene, 25 °C.

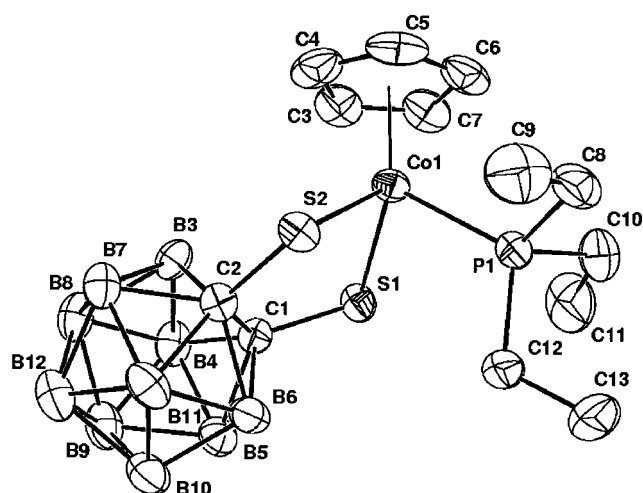


Figure 4. Molecular structure of **4b** with atom labeling; ellipsoids show 30% probability levels, and hydrogen atoms have been omitted for clarity.

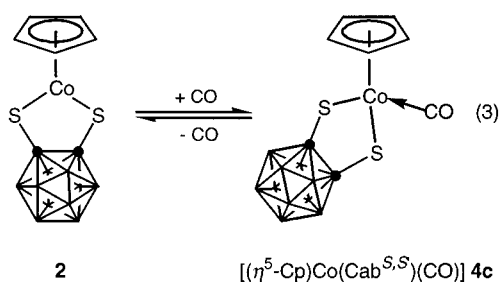
4a,b were prepared from the reaction between the monomeric cobalt complex **2** and a slight excess of the corresponding nucleophiles such as CNBu^t and PEt₃ (Scheme 2).

Isolation of the pure products, which ranged from yellow to red, was achieved by recrystallization. Typically, the yields of **4a,b** were on the order of 92–95%. The structure of **4a,b** was determined on the basis of NMR spectroscopy and IR spectra, as well as elemental analysis. Thus, complex **4a** exhibited a single CN stretching absorption at 2208 cm⁻¹ in the IR spectrum, and this wavenumber is normal for a terminal Co–CNR ligand and significant π -back-bonding of the isocyanide ligand. The ¹H NMR spectrum of **4a** indicated a singlet signal at δ 1.59 due to a *tert*-butyl moiety.

The ³¹P{¹H} NMR of **4b** exhibited a singlet signal at δ 37.19. ¹H NMR data for **4b** conform to the structure determined by the X-ray structural study. The structure of **4b** is closely related to the phosphine adducts of the iridium thiolato complex $[(\eta^5\text{-Cp}^*)\text{Ir}(\text{Cab}^{\text{S,S}})(\text{PMe}_3)]$.^{5c} The ORTEP diagram in Figure 4 shows the molecular

structure of **4b** and confirms the six-coordinate geometry about the cobalt atom, assuming that the cyclopentadienyl ring serves as a three-coordinate ligand. The molecule possesses idealized *C_s* molecular symmetry, as is commonly observed with many three-legged piano-stool complexes. Complex **4b** has similar Co–S bond lengths of Co(1)–S(1) 2.2548(5) Å and Co(1)–S(2) 2.2609(6) Å, respectively, in good agreement with the existing values in the literature for a wide variety of Co–S σ bonds. In addition, the Co–S distance (2.2579(6) (av) Å) of complex **4b** at the formally 18-electron cobalt center is significantly longer than that (2.113(2) (av) Å) of complex **1**.¹⁰ This difference in bond length may be attributed to π -orbital donation of the lone pairs from the sulfur atoms to the electron-deficient cobalt center of complex **2**. The Co–S bond lengths (2.2579(6) (av) Å) and S(1)–Co(1)–S(2) bond angle (91.59(2)°) in **4b** can be compared with the corresponding parameters in $[(\text{Cp})\text{Co}(\text{S}_2\text{C}_2(\text{COOMe})_2(\text{COOMe})_2)(\text{P}(\text{OMe})_3)]$ (2.231(1) (av) Å and 90.26(5)°).¹⁷ The Co atom environment is transformed from a two-legged piano-stool geometry in **2** to a three-legged version in **4b**. The Cp ring undergoes tilting of about 54.40(7)° relative to the [S(1), Co(1), S(2)] plane when **2** converts to **4b**, whereas in **1** the metallocycle is nearly planar (max. dev. = 0.1 Å for **1**) and folding occurs in **4b** along the S(1)–S(2) vector. A dihedral angle of 28.28(5)° relates the [S(1), Co(1), S(2)] and [S(1), C(1), C(2), S(2)] planes in **4b**.

Treatment of **2** with an atmospheric pressure of carbon monoxide in toluene resulted in the formation of the mononuclear carbonyl adduct $[(\eta^5\text{-Cp})\text{Co}(\text{Cab}^{\text{S,S}})(\text{CO})]$ (**4c**). Reaction of **2** with an excess of carbon monoxide at room temperature proceeded smoothly, monitored by the change in the red color of the solution to yellow. Complex **4c** consists of a carbonyl, a cyclopentadienyl ligand, and a dithiolate ligand, proven by spectroscopic means. The structure of **4c** was determined on the basis of spectral data as well as elemental analysis. The ¹H NMR spectrum of **4c** exhibited a single proton signal assignable to a coordinated cyclopentadienyl ligand. The IR spectrum indicates that one carbon monoxide is bound to the cobalt atom, in accordance with the strong $\nu(\text{CO})$ band at 1965 cm⁻¹. It is interesting to note that a reversible 16–18-electron interconversion is present as shown in eq 3. Thus, carbonylation



of a toluene solution of **2** gave **4c**, while a nitrogen purge reverses this reaction. This finding suggests that CO coordination competes with S-to-Co π donation in **2**, an issue that will be subjected to further investigation.

Electrochemical Studies on 18-Electron Metal Complexes $[(\eta^5\text{-Cp})\text{Co}(\text{Cab}^{\text{S,S}})(\text{L})]$ (L = CNBu^t (4a**), PEt₃ (**4b**)).** Figure 5B,C displays cyclic voltammograms of $[(\eta^5\text{-Cp})\text{Co}(\text{Cab}^{\text{S,S}})(\text{CNBu}^t)]$ (**4a**) and $[(\eta^5\text{-Cp})\text{Co}(\text{Cab}^{\text{S,S}})(\text{PEt}_3)]$ (**4b**) in CH₂Cl₂ containing 0.1 M TBAB,

(18) Herberhold, M.; Jin, G.-X.; Yan, H.; Milius, W.; Wrackmeyer, B. *J. Organomet. Chem.* **1999**, *587*, 252.

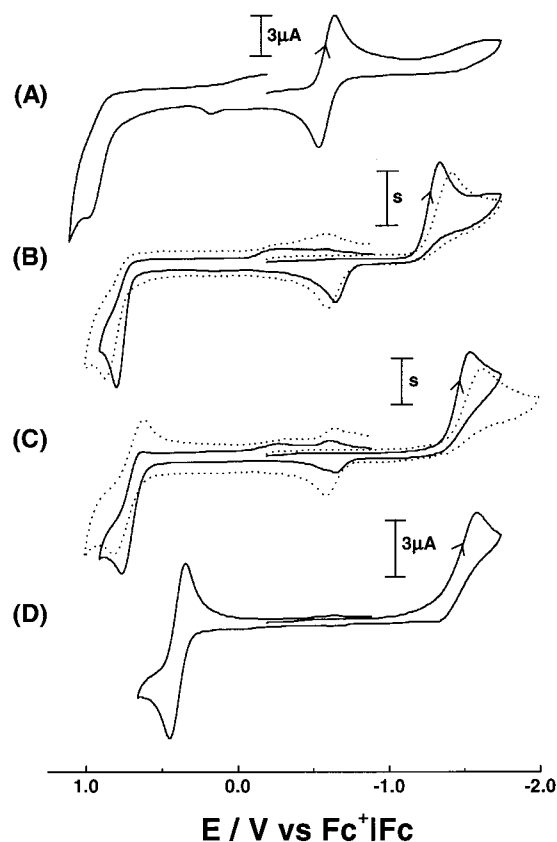


Figure 5. Cyclic voltammograms of 1 mM $[(\eta^5\text{-Cp})\text{Co}(\text{Cab}^{S,S})]$ (**2**) (A), $[(\eta^5\text{-Cp})\text{Co}(\text{Cab}^{S,S})(\text{CNBu}^9)]$ (**4a**) (B), $[(\eta^5\text{-Cp})\text{Co}(\text{Cab}^{S,S})(\text{PEt}_3)]$ (**4b**) (C), and $[(\eta^5\text{-Cp})\text{Co}(\text{Cab}^{S,S})(\eta^1\text{-CH}_2\text{SiMe}_3\text{-S})]$ (**5**) (D) at a platinum disk electrode with negative initial scan direction; in CH_2Cl_2 containing 0.1 M TBAB; $\nu = 0.1 \text{ V s}^{-1}$ (solid line) or 1.0 V s^{-1} (broken line). The scale bar corresponding to the solid and broken line waves is 3.0 and $10.0 \mu\text{A}$, respectively.

where the scan rates (ν) of CVs of solid and broken lines are 0.1 and 1.0 V s^{-1} , respectively. The CV of **4a** exhibits two major redox responses, i.e., 0/−1 ($E_{\text{pc}} = -1.34 \text{ V}$) and +1/0 ($E_{\text{pa}} = 0.80 \text{ V}$), which are not reversible (Figure 5B). Figure 5C displays the CV scan of **4b**, which is very similar to that of **4a** except for the position of the redox potentials, i.e., $E_{\text{pc}} = -1.53 \text{ V}$ for 0/−1 and $E_{\text{pa}} = 0.77 \text{ V}$ for +1/0. However, an increased scan rate by 10-fold (broken line) leads to significant improvement in the reversibility of the +1/0 redox couple of **4b** compared with that of **4a**.

Another small reversible peak near -0.60 V in the CVs of **4a** and **4b** is of interest in this study because its redox potential is very close to that of the 0/−1 couple in the CV of **2**. Note, however, that this small peak is not observed in the CVs of **4a** and **4b** with a potential scan range between -1.0 and 0.2 V . Judging from the position of the redox potential and the quasi-reversibility of the oxidation,¹⁹ this small wave is the reduction wave of the 16-electron complex **2**. It is probable that **4a,b** slowly eliminated the Lewis bases and regenerated the mononuclear cobalt complex **2**. No further effort was expended to clarify the small anodic peak near -0.2 V .

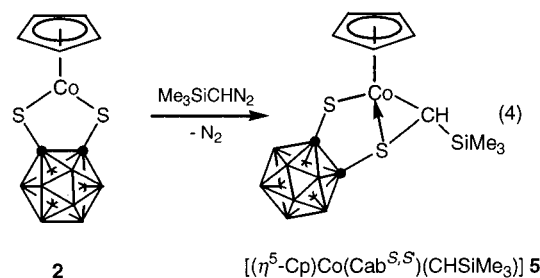
The results allow the following major conclusions to be drawn: Both the reduction and oxidation potentials of the 18-electron complexes **4a,b** shifted to a more negative side than those of the 16-electron complex **2**. That is, both metal and sulfur atoms became electron-

rich by the addition of Lewis bases. Furthermore, reversible cathodic redox steps can become irreversible (**2** vs **4a,b**) because reductions become more difficult. However, increased scan rates (1.0 V s^{-1}) lead to a significant improvement in the stability of the 0/+1 redox couple in **4b**. This trend is consistent with a greater stabilization of the 0/+1 redox couple by the ancillary phosphine ligand, because it is known that phosphine is a stronger σ -donor relative to isocyanide.

Reaction of **2** with (Trimethylsilyl)diazomethane.

It is recognized that π donation by a lone pair of electrons on the coordinated sulfur atom alleviates such electron deficiency, and thus the coordinative unsaturation occurs around the transition-metal center. Consequently, this geometry suggests that some of the multiple-bond character is present in the Co–S bonds of complex **2**. To verify the nature of the Co–S bonds, the addition reaction of a diazomethane to **2** has been investigated.

The reaction of **2** with trimethylsilyl diazomethane in methylene chloride solution at room temperature for 1 h gave the trimethylsilyl methylene adduct **5** in 84% (eq 4). The composition of the new complex **5** is unequivocally established by elemental analysis.



Complex **5** was isolated as an air-stable microcrystalline solid and was spectroscopically characterized. Complex **5** shows the expected ^1H and ^{13}C NMR signals. Thus, the ^1H NMR spectrum of complex **5** exhibits resonances for a Cp ligand at $\delta 4.99$, a trimethylsilyl group at $\delta 0.24$, and methine proton at $\delta 3.49$. The ^{13}C NMR spectrum also corresponds to the Co–S-inserted structure: alkenyl carbons of the Cp ring and carbon atoms of the Co–S-substituted trimethylsilyl methine unit.

To establish the exact conformation of the adduct, the structure of **5** was determined by single-crystal X-ray analysis. The molecular structure of **5** is shown in Figure 6. Selected bond lengths and bond angles are given in Tables 2 and 3. The X-ray structure of **5** shows that the cobalt assumes a three-legged piano-stool configuration with a bicyclic metallacyclic ring. This is due to the insertion of the coordinated dithiolato ligand at the cobalt(III) metal center. The five Co, S, C, C, and S atoms comprising the central skeleton of the molecule are all nearly coplanar, with a dihedral angle of $83.0(1)^\circ$ between the planes defined by $[\text{Co}(1), \text{S}(1), \text{C}(1), \text{C}(2), \text{S}(2)]$ and $[\text{Co}(1), \text{S}(2), \text{C}(8)]$. In **5**, the trimethylsilyl group is located in the anti-position with respect to the cobaltadithia-*o*-carborane ring. The formation of a methylene bridge between a metal and a chalcogen in a reaction with a diazoalkane compound is a typical result due to unsaturation.²⁰ These cycloaddition reactions suggest that a certain degree of multiple-bond character is present in the Co–S bond of complex **2**.

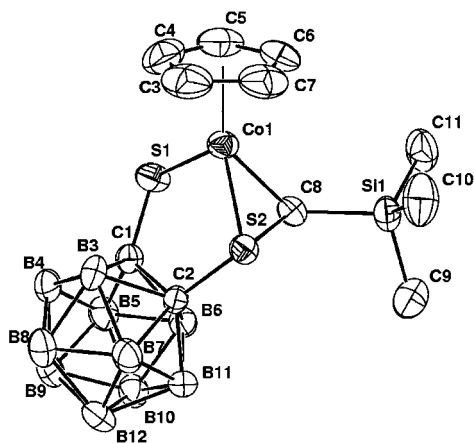
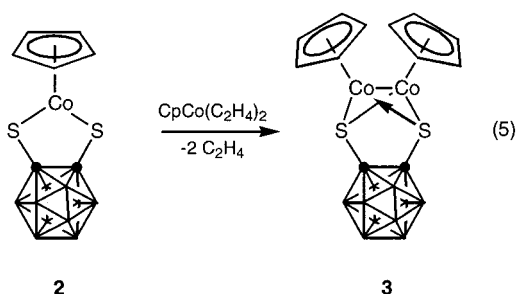


Figure 6. Molecular structure of **5** with atom labeling; ellipsoids show 30% probability levels, and hydrogen atoms have been omitted for clarity.

Electrochemical Studies of 5. Figure 5D displays the CV scans of **5**. Unlike **4a,b**, the alkylidene-bridged complex **5** exhibits a well-defined reversible one-electron oxidation wave at $E_{1/2} = 0.40$ V, which is more positive than those of **4a,b** by >0.3 V. The reversible one-electron oxidation waves of **5** are ascribed to the oxidation of the dithiolene sulfur atoms. Note that the small redox peak near -0.60 V, i.e., elimination of the Lewis base, is hardly observed, unlike the CVs of **4a,b**. Thus, the CV behavior is consistent with greater stability of the alkylidene-bridged complex that may involve the coordination of the tridentate *S,S,C*-ligand system.

Addition of Co–S Bonds of 2. Similar to the reactions between **2** and a diazoalkane, the cobaltadithia-*o*-carborane ring in **2** undergoes the addition of an alkyne group between Co and S in its reaction with alkynes. The reaction of **2a** with 1 equiv of $[\text{CpCo}(\text{C}_2\text{H}_4)_2]$ in toluene at -78 °C proceeded smoothly, as monitored by the change of the red solution to green (eq 5).

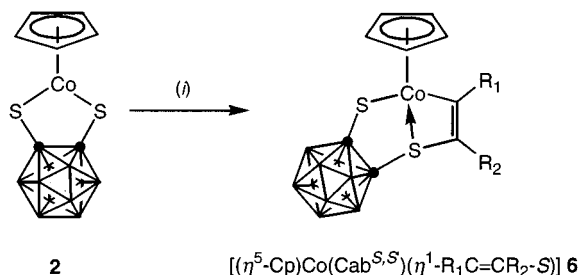


The green complex $[(\eta^5\text{-Cp})\text{Co}]_2(\text{Cab}^{S,S})$ (**3**) was isolated in 90% yield as a crystalline solid after precipitation from toluene/hexane. The spectral data for **3** were identical with those of the authentic samples.

(19) Takayama, C.; Takeuchi, K.; Ohkoshi, S.; Janario, G. C.; Sugiyama, T.; Kajitani, M.; Sugimori, A. *Organometallics* **1999**, *18*, 2843.

(20) (a) Takayama, C.; Takeuchi, K.; Kajitani, M.; Sugiyama, T.; Sugimori, A. *Chem. Lett.* **1998**, 241. (b) Sakurada, M.; Kajitani, M.; Dohki, K.; Akiyama, T.; Sugimori, A. *J. Organomet. Chem.* **1992**, *423*, 141. (c) Sakurada, M.; Okubo, J.; Kajitani, M.; Akiyama, T.; Sugimori, A. *Phosphorus, Sulfur, Silicon, Relat. Elements* **1992**, *67*, 145. (d) Kajitani, M.; Sakurada, M.; Dohki, K.; Suetsugu, T.; Akiyama, T.; Sugimori, A. *J. Chem. Soc., Chem. Commun.* **1990**, 19. (e) Sakurada, M.; Okubo, J.; Kajitani, M.; Akiyama, T.; Sugimori, A. *Chem. Lett.* **1990**, 1837.

Scheme 3. Addition Reaction of 16-Electron Metal Complexes **2**^a



^a Legend: (i) R_1CCR_2 , toluene, 110 °C ($\text{R}_1 = \text{R}_2 = \text{MeOCO}$ **a**; $\text{R}_1 = \text{H}$, $\text{R}_2 = \text{Ph}$ **b**; $\text{R}_1 = \text{H}$, $\text{R}_2 = \text{SiMe}_3$ **c**).

Complex **2** was found to be a good precursor for other addition reactions. Thus, treatment of **2** with 1–2 equiv of an alkyne in refluxing benzene for 2 h gave novel alkyne adduct complexes, $[(\eta^5\text{-Cp})\text{Co}(\text{Cab}^{S,S})(\eta^1\text{-R}_1\text{C}=\text{CR}_2\text{-S})]$ (**6**; $\text{R}_1 = \text{R}_2 = \text{COOMe}$ (**6a**); $\text{R}_1 = \text{H}$, $\text{R}_2 = \text{Ph}$ (**6b**); $\text{R}_1 = \text{H}$, $\text{R}_2 = \text{SiMe}_3$ (**6c**)), in moderate yield (Scheme 3). Isolation of the pure products was achieved by recrystallization. Typically, the yields of **6** were on the order of 23–91%. Although the process outlined in Scheme 3 proved quite general, there were, however, structural limitations observed for the metallabicyclic complexes **6**. For example, several attempts to synthesize the complexes **2** with electron-rich acetylenes such as dialkylated and silylated acetylenes were unsuccessful, yielding only decomposition under prolonged reflux conditions. Conversion of **2** to the corresponding metallabicyclic complexes **6** is generally favored by electron-deficient alkynes. Indeed, compounds **6a,b** were produced in high yields from the direct two-carbon insertion reaction of electron-deficient alkynes with complex **2**.

Adducts **6a–c** were isolated as air-stable, microcrystalline solids and were spectroscopically characterized. Each of the adducts shows the expected ^1H and ^{13}C NMR signals and is a 1:1 adduct of the cobaltadithia-*o*-carborane and alkene groups by elemental analyses. The IR spectra of **6a–c** exhibit one $\nu(\text{C}=\text{C})$ stretching band, and the ^1H NMR spectra of **6a–c** display the characteristic resonances of a coordinated olefin. The ^1H NMR spectrum of adduct **6a** showed two nonequivalent ^1H signals of the OMe groups of the ester and two nonequivalent ^{13}C signals of the ester CO groups, in agreement with the molecular structure of this adduct as determined by single-crystal X-ray analysis (Figure 7). The ^1H NMR spectrum of **6b** shows the terminal proton at δ 2.36 and multiplet signals (δ 7.30) of the phenyl group of the acetylene. For **6c**, the SiMe_3 groups of the olefin give rise to a singlet centered at δ 0.29. For the $^{13}\text{C}\{^1\text{H}\}$ NMR spectra of **6a–c**, it is sufficient to point out that the resonances due to the π -bound olefin carbons are characteristically upfield-shifted. The spectroscopic data of the cobalt complexes are in complete agreement with the proposed structure of **6a–c**.

To provide structural information for one of the new compounds prepared, a single-crystal X-ray diffraction study of the dimethyl acetylenedicarboxylate insertion product **6a** was undertaken. Figure 7 and Tables 2 and 3 show the ORTEP drawing and selected bond distances and bond angles, respectively. The structural analysis of **6a** indeed authenticated the insertion of the coordinated dithiolato ligand at the cobalt(III) metal center.

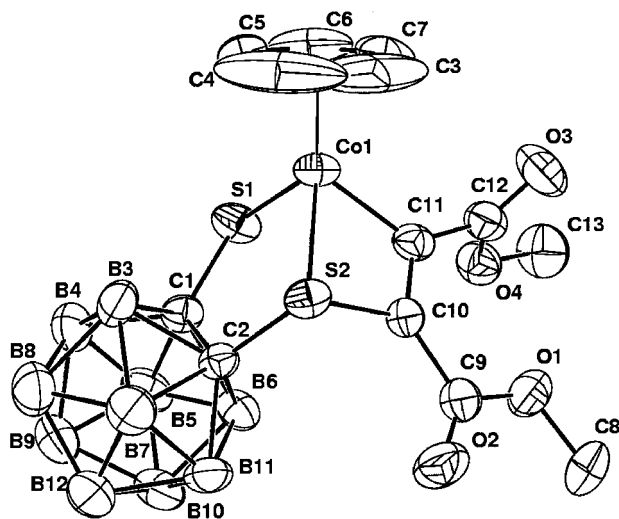


Figure 7. Molecular structure of **6a** with atom labeling; ellipsoids show 30% probability levels, and hydrogen atoms have been omitted for clarity.

In addition, **6a** shows a puckering of the five-membered cobaltadithiolene ring in **2**, resulting in the olefinic carbon atoms being brought closer to the metal center, possibly in an effort to relieve its steric repulsion. It is also possible that a better overlap of the alkenyl moiety with the cobalt metal center is responsible for such a puckering of the cobaltadithiolene ring. This structure results from the addition of R_1CCR_2 into the Co–S bond of **2**. Thus, **6a** adopts a three-legged piano-stool conformation with S(1), S(2), and the olefin C(1)–C(2) moiety as the legs. The olefin moiety of the dithiolato ligand is bonded unsymmetrically to the metal center, with the Co(1)–C(11) being 1.912(5) Å. In adduct **6a**, the alkene moiety thus formed bridges between Co and S of the metalladithia-*o*-carborane ring without breaking the Co–S bond [Co(1)–S(1) = 2.247(2) Å, Co(1)–S(2) = 2.246(1) Å]. This adduct has a piano-stool structure consisting of a four-membered and a five-membered ring. The central metal is coordinatively saturated, in contrast to the pentacoordinate structure of complex **2**. In this adduct, the plane of the C(11)–Co(1)–S(2)–C(10) four-membered ring is almost perpendicular to the plane of the almost planar dithia-*o*-carborane ring. The bond length of C(10)–C(11) (1.340(7) Å) is slightly longer than the typical value for the carbon–carbon double bond and agrees with the normal metal olefin C=C bond length. Such an addition of an alkyne into an M–S bond has been observed in Sugimori's work on the chemo selective addition of dimethyl acetylenedicarboxylate to the Rh–S bond in a rhodium-catalyzed reaction.²¹ It was also observed that a series of novel alkyne addition reactions^{5a,22} via cyclometalation or isomerization is favored in the case of the corresponding rhodium and iridium dithiolates with a bulky Cp* ancillary ligand.

Conclusions

This paper demonstrates the rich structural chemistry possible for the *o*-carboranyl dithiolate ligand; three

(21) (a) Kajitani, M.; Suetsugu, T.; Takagi, T.; Akiyama, T.; Sugimori, A.; Aoki, K.; Yamazaki, H. *J. Organomet. Chem.* **1995**, *487*, C8. (b) Sakurada, M.; Kajitani, M.; Dohki, K.; Akiyama, T.; Sugimori, A. *J. Organomet. Chem.* **1992**, *423*, 141. (c) Kajitani, M.; Suetsugu, T.; Wakabayashi, R.; Igarashi, A.; Akiyama, T.; Sugimori, A. *J. Organomet. Chem.* **1985**, *293*, C15.

bonding modes are presented in eqs 2 and 4 and Scheme 2. The results demonstrate the versatility of the coordinatively unsaturated half-sandwich organometallic reagents in exploring the chemistry of the five-membered cobaltadithiolene ring.

The results observed in this work can be rationalized in the following qualitative but self-consistent manner. The easy oxidation of **2** establishes its electron-rich character. As a metalladithiolene derivative, **2** is stabilized by the π donation from the filled $p\pi$ orbital of the sulfur atoms to the empty $d\pi$ orbital of the cobalt atom. When such complexes are oxidized, orbitals contract and the π -donor ability of the *o*-carboranyl dithiolato ligand is diminished. To compensate for the weakened S to Co π interaction, the metal center in **2** adopts a favorable σ -Co–Co interaction, which leads to transformation of **2** to give **3**. In addition, complex **III** demonstrates that the steric bulk of the pentamethylcyclopentadienyl group plays an important role in the type of reaction. Increasing bulkiness of the pentamethylcyclopentadienyl ligand in **III** hampers the formation of the bimetallic complexes as found in **3** and instead favors the formation of mononuclear complexes.

Because **2** is a 16-electron coordinatively unsaturated species, it is clear that this compound exhibits remarkable reactivity toward various Lewis bases such as CNBu^t and PEt₃. In addition, Complex **2** exhibits some coordinative unsaturation and thus is susceptible to the addition of organic and organometallic compounds into the Co–S bond of **2**.

Experimental Section

General Procedures. All manipulations were performed under a dry, oxygen-free, nitrogen or argon atmosphere using standard Schlenk techniques or in a Vacuum Atmosphere HE-493 drybox. THF was freshly distilled over potassium benzophenone. Toluene was dried and distilled from sodium benzophenone. Dichloromethane and hexane were dried and distilled over CaH₂. ¹³C, ¹H, ¹¹B, and ³¹P NMR spectra were recorded on a Varian Gemini 2000 spectrometer operating at 50.3, 200.1, 64.2, and 80.0 MHz, respectively. All proton and carbon chemical shifts were measured relative to internal residual benzene from the lock solvent (99.5% C₆D₆) and then referenced to Me₄Si (0.00 ppm). Chemical shifts were reported (δ , ppm) from external boron trifluoride diethyl etherate for ¹¹B spectroscopy. The ³¹P NMR spectra were recorded with 85% H₃PO₄ as an external standard. IR spectra were recorded on a Biorad FTS-165 spectrophotometer. Elemental analyses were performed with a Carlo Erba Instruments CHNS-O EA1108 analyzer. All melting points were uncorrected. High-resolution mass spectra were obtained on a VG Micromass 7070H mass spectrometer. All the electrochemical measurements were carried out in CH₂Cl₂ or CH₃CN solutions containing 1.0 mM metal complex and 0.1 M tetrabutylammonium fluoroborate (TBAB) or tetrabutylammonium perchlorate (TBAP), respec-

(22) (a) Herberhold, M.; Yan, H.; Milius, W.; Wrackmeyer, B. *J. Chem. Soc., Dalton Trans.* **2001**, 1782. (b) Herberhold, M.; Yan, H.; Milius, W.; Wrackmeyer, B. *J. Organomet. Chem.* **2001**, *623*, 149. (c) Herberhold, M.; Yan, H.; Milius, W.; Wrackmeyer, B. *Organometallics* **2000**, *19*, 4289. (d) Herberhold, M.; Yan, H.; Milius, W.; Wrackmeyer, B. *J. Organomet. Chem.* **2000**, *604*, 170. (e) Herberhold, M.; Yan, H.; Milius, W.; Wrackmeyer, B. *Chem. Eur. J.* **2000**, *6*, 3026. (f) Herberhold, M.; Yan, H.; Milius, W.; Wrackmeyer, B. *Z. Anorg. Allg. Chem.* **2000**, *626*, 1627. (g) Herberhold, M.; Yan, H.; Milius, W.; Wrackmeyer, B. *Angew. Chem., Int. Ed.* **1999**, *38*, 3689. (h) Herberhold, M.; Jin, G.-X.; Yan, H.; Milius, W.; Wrackmeyer, B. *Eur. J. Inorg. Chem.* **1999**, 873. (i) Herberhold, M.; Jin, G.-X.; Yan, H.; Milius, W.; Wrackmeyer, B. *J. Organomet. Chem.* **1999**, *587*, 252.

tively, at room temperature using a BAS 100B electrochemical analyzer. A platinum disk (dia. 1.6 mm) and platinum wire were used as working and counter electrodes. The reference electrode used was Ag|AgNO₃, and all the potential values shown were calibrated vs the Fc⁺|Fc redox couple, unless otherwise specified. E_{pa} (anodic peak potential) and E_{pc} (cathodic peak potential) were used for the redox waves; these lack reversibility. The $E_{1/2}$ value indicated is the average of E_{pa} and E_{pc} for the reversible redox waves.

o-Carborane was purchased from the Katechem and used without purification. Complex Cab^{S,S'} (**1**),²³ CpCo(CO)I₂,²⁴ Cp*Co(CO)I₂,²⁴ [Cp*RhCl₂]₂,²⁵ and [Cp*IrCl₂]₂²⁶ were prepared according to literature methods.²⁴

Preparation of [(η^5 -Cp)Co(Cab^{S,S'})] (2**).** Representative procedure: A 3.2 mmol solution of **1** in THF (20 mL) was added to a stirred solution of CpCo(CO)I₂ (1.22 g, 3.0 mmol) in THF (30 mL) cooled to -78 °C. The reaction mixture was then allowed to react at 0 °C for 1 h, and the solution was stirred for another 2 h at room temperature. The solution gradually turned dark red, suggesting the formation of an *o*-carboranyl dithiolato metal complex. The solution was reduced in vacuo to about half its original volume, and some insoluble material was removed by filtration. The solution was removed under vacuum, and the resulting residue was taken up in a minimum of methylene chloride and then transferred to a column of silica gel. The crude residue was purified by column chromatography, affording >98% pure complex as red crystals. Colorless crystals of **2** were formed in 83% yield (0.83 g, 2.5 mmol). Data for **2**. Anal. Calcd for C₇H₁₅B₁₀S₂Co: C, 25.45; H, 4.58. Found: C, 25.51; H, 4.63. IR (KBr, cm⁻¹): ν (B-H) 2554. ¹H NMR (200.13 MHz, ppm, CDCl₃): 5.26 (s, 5H, Cp). ¹³C{¹H} NMR (50.3 MHz, ppm, CDCl₃): 81.81 (s, Cp).

Synthesis of the Cobalt, Rhodium, and Iridium Thioloates III–V. [(η^5 -Cp*)Co(Cab^{S,S'})] (III**).** **III** was prepared from 3.0 mmol of Cp*Co(CO)I₂. After flash chromatography on silica gel with hexane/CHCl₃ (90/10), **III** (43%) was isolated as an orange solid. ¹H NMR (200.13 MHz, ppm, CDCl₃): 1.65 (s, 15H, Cp*).

[(η^5 -Cp*)Rh(Cab^{S,S'})] (IV**).** **IV** was prepared from 1.5 mmol of [Cp*RhCl₂]₂. After flash chromatography on silica gel with hexane/CHCl₃ (90/10), **IV** (67%) was isolated as a green solid. ¹H NMR (200.13 MHz, ppm, CDCl₃): 1.79 (s, 15H, Cp*).

[(η^5 -Cp*)Co(Cab^{S,S'})] (V**).** **V** was prepared from 1.5 mmol of [Cp*IrCl₂]₂. After flash chromatography on silica gel with hexane/CHCl₃ (90/10), **V** (86%) was isolated as a blue solid. ¹H NMR (200.13 MHz, ppm, CDCl₃): 1.87 (s, 15H, Cp*).

Reaction of **2 with BH₃·THF.** A 0.66 g amount of **2** (2.0 mmol) was dissolved in 30 mL of dry THF and cooled to -78 °C. A 10 mL portion of 1.0 M BH₃·THF solution (10.0 mmol) was added with stirring over 30 min, and the solution was allowed to warm to room temperature. The red solution turned dark green as the solution warmed. The solution was filtered in air, and the solvent was removed under reduced pressure. The resultant residue was extracted with 60 mL of hexane and reduced to 10 mL. Cooling at -30 °C overnight gave a yellow solid, which was dried under vacuum, recrystallized from cold hexane, and characterized as **D** (0.13 g, 0.60 mmol, 30%), mp 48–50 °C. HRMS for ¹¹B₁₁¹²C₂¹H₁₁³²S₂ (*m/e*): calcd, 220.1326; found 220.1334. IR (KBr, cm⁻¹): ν (cage B-H) 2600, ν (exo-cyclic B-H) 2495, ν (B-S) 795, ν (B-H) 730. ¹¹B NMR (64.2 MHz, ppm, CDCl₃): 11.89 (d, J_{B-H} = 160 Hz, S₂BH).

The remaining solid was passed through a short column of silica gel with CH₂Cl₂ as the eluent. A 0.43 g amount of **3** was obtained after removal of the solvent (0.95 mmol, 47% yield). Data for **3**. Anal. Calcd for C₁₂H₂₀B₁₀S₂Co₂: C, 31.72; H, 4.44. Found: C, 31.69; H, 4.49. IR (KBr, cm⁻¹): ν (B-H) 2586. ¹H

NMR (200.13 MHz, ppm, CDCl₃): 5.00 (s, 5H, Cp). ¹³C{¹H} NMR (50.3 MHz, ppm, CDCl₃): 77.79 (s, Cp).

Reaction of **2 with CNBu^t.** Under argon, CNBu^t (0.23 mL, 2.0 mmol) was added to a stirred solution of complex **2** (0.33 g, 1.0 mmol) in toluene (10 mL) cooled to 0 °C. The red solution immediately turned yellow. After stirring for 30 min, the solution was evaporated to dryness. The yellow residue of **4a** was dried in vacuo. Yield: 0.38 g (0.92 mmol, 92%). Data for **4a**. Anal. Calcd for C₁₂H₂₄B₁₀S₂CoN: C, 34.86; H, 5.85; N, 3.39. Found: C, 34.90; H, 5.81; N, 3.45. IR (KBr, cm⁻¹): ν (B-H) 2595, ν (B-H) 2569, ν (C=N) 2208. ¹H NMR (200.13 MHz, ppm, CDCl₃): 5.27 (s, 5H, Cp), 1.59 (s, 9H, NBu^t). ¹³C{¹H} NMR (50.3 MHz, ppm, CDCl₃): 89.03 (s, Cp), 30.42 (s, NBu^t).

Reaction of **2 with PEt₃.** Under argon, PEt₃ (0.30 mL, 2.0 mmol) was added to a red solution of complex **2** (0.33 g, 1.0 mmol) in 10 mL of methylene chloride. The resultant yellow solution was stirred for 30 min and evaporated to dryness. The yellow residue of **4b** was dried in vacuo. Yield: 0.43 g (0.95 mmol, 95%). Data for **4b**. Anal. Calcd for C₁₃H₃₀B₁₀S₂CoP: C, 34.81; H, 6.74. Found: C, 34.90; H, 6.81. IR (KBr, cm⁻¹): ν (B-H) 2592, ν (B-H) 2583, ν (P-C) 1035. ¹H NMR (200.13 MHz, ppm, CDCl₃): 5.14 (s, 5H, Cp), 1.97 (dq, 6H, PCH₂), 1.07 (dt, 9H, PCH₂Me). ¹³C{¹H} NMR (50.3 MHz, ppm, CDCl₃): 88.47 (s, Cp), 18.70 (d, ¹J_{P-C} = 29 Hz, P(CH₂Me)₃), 7.68 (s, P(CH₂Me)₃). ³¹P{¹H} NMR (80.0 MHz, ppm, CDCl₃): 37.19 (s, PEt₃).

Reaction of **2 with CO.** A solution of complex **2** (0.33 g, 1.0 mmol) in toluene (20 mL) was treated with excess CO gas at room temperature for 5 min. The red color of the solution quickly faded to give a yellow solution. The volatile substances were then removed in vacuo, and the resulting solid was extracted with CH₂Cl₂. Addition of hexane to the concentrated extract gave complex **4c** as yellow-orange crystals. Yield: 0.30 g (0.84 mmol, 84%). Data for **4a**. Anal. Calcd for C₈H₁₅B₁₀S₂-CoO: C, 26.81; H, 4.22. Found: C, 26.93; H, 4.30. IR (KBr, cm⁻¹): ν (B-H) 2587, ν (CO) 2077. ¹H NMR (200.13 MHz, ppm, CDCl₃): 5.52 (s, 5H, Cp). ¹³C{¹H} NMR (50.3 MHz, ppm, CDCl₃): 237.43 (s, CO), 78.59 (s, Cp).

Reaction of **2 with Me₃SiCHN₂.** A solution of complex **2** (0.33 g, 1.0 mmol) in toluene (20 mL) was treated with a 2.0 M hexane solution of (trimethylsilyl)diazomethane (0.6 mL, 1.2 mmol) at room temperature for 5 min. The red color of the solution quickly faded to give a yellow solution. The volatile substances were then removed in vacuo, and the resulting solid was extracted with CH₂Cl₂. Addition of hexane to the concentrated extract gave complex **5** as yellow-orange crystals. Yield: 0.35 g (0.84 mmol, 84%). Data for **5**. Anal. Calcd for C₁₁H₂₅B₁₀S₂CoSi: C, 31.72; H, 6.05. Found: C, 31.77; H, 6.09. IR (KBr, cm⁻¹): ν (B-H) 2596, ν (B-H) 2568. ¹H NMR (200.13 MHz, ppm, CDCl₃): 4.99 (s, 5H, Cp), 3.49 (s, 1H, Me₃SiCH), 0.24 (s, 9H, SiMe₃). ¹³C{¹H} NMR (50.3 MHz, ppm, CDCl₃): 83.10 (s, Cp), 49.93 (s, Me₃SiCH), 0.00 (s, SiMe₃).

General Synthesis of [(η^5 -Cp)Co(Cab^{S,S'})(L)] [η^1 -R₁C=CR₂-S (6**; R₁ = R₂ = COOMe (**6a**); R₁ = H R₂ = Ph (**6b**); R₁ = H R₂ = SiMe₃ (**6c**))].** In a typical run **2** (0.33 g, 1.0 mmol) and alkynes were dissolved in toluene (15 mL) under argon, and the solution was stirred for 8 h at room temperature. The red color of the solution slowly faded to give a yellow solution, suggesting the formation of an adduct. The completion of the reaction was monitored by TLC. The solution was reduced in vacuo to about half its original volume, and some insoluble material was removed by filtration. Addition of hexane to the resulting solution afforded **6** as a dark yellow precipitate.

Analytical Data for **6a.** **6a** was prepared from 2.0 mmol (0.25 mL) of dimethyl acetylenedicarboxylate. After recrystallization from toluene, **6a** (0.43 g, 0.91 mmol, 91% yield) was isolated as a yellow solid. Anal. Calcd for C₁₃H₂₁B₁₀S₂CoO₄: C, 33.05; H, 4.48. Found: C, 33.10; H, 4.52. IR (KBr, cm⁻¹): ν (B-H) 2580, ν (CO) 1710, ν (C=C) 1579. ¹H NMR (200.13 MHz, ppm, CDCl₃): 5.23 (s, 5H, Cp), 3.94 (s, 3H, OMe), 3.77 (s, 3H, OMe). ¹³C{¹H} NMR (50.3 MHz, ppm, CDCl₃): 171.07 (s,

(23) Smith, H. D., Jr.; Obenland, C. O.; Papetti, S. *Inorg. Chem.* **1966**, *5*, 1013.

(24) Frith, S. A.; Spencer, J. L. *Inorg. Synth.* **1990**, *28*, 273.

(25) Gassman, P. G.; Mickelson, J. W.; Sowa, J. R., Jr. *Inorg. Synth.* **1997**, *31*, 236.

MeOCO), 155.25 (s, MeOCO), 118.84 (s, MeOCOC=), 98.40 (s, MeOCOC=), 86.70 (s, Cp), 52.85 (s, OMe), 52.71 (s, OMe).

Analytical Data for 6b. **6b** was prepared from 2.0 mmol (0.22 mL) of phenylacetylene. After recrystallization from toluene, **6b** (0.38 g, 0.88 mmol, 88% yield) was isolated as a yellow solid. Anal. Calcd for C₁₅H₂₁B₁₀S₂Co: C, 41.66; H, 4.89. Found: C, 41.73; H, 4.95. IR (KBr, cm⁻¹): ν(B-H) 2600, ν(C=C) 1488, ν(C=C) 1442. ¹H NMR (200.13 MHz, ppm, CDCl₃): 7.30 (s, 5H, Ph), 4.51 (s, 5H, Cp), 2.36 (s, 1H, C=CH). ¹³C{¹H} NMR (50.3 MHz, ppm, CDCl₃): 192.05 (s, HC=CPh), 176.64 (s, HC=CPh), 127.58 (m, Ph), 86.70 (s, Cp).

Analytical Data for 6c. **6c** was prepared from 1.0 mmol (0.28 mL) of trimethylsilyl acetylene. After recrystallization from toluene, **6c** (0.10 g, 0.23 mmol, 23% yield) was isolated as a yellow solid. Anal. Calcd for C₁₂H₂₅B₁₀S₂CoSi: C, 33.63; H, 5.88. Found: C, 33.68; H, 5.93. IR (KBr, cm⁻¹): ν(B-H) 2586, ν(CO) 1401. ¹H NMR (200.13 MHz, ppm, CDCl₃): 5.00 (s, 5H, Cp), 1.91 (s, 1H, C=CH), 0.29 (s, 9H, SiMe₃). ¹³C{¹H} NMR (50.3 MHz, ppm, CDCl₃): 146.51 (s, HC=CSiMe₃), 77.92 (s, Cp), 1.78 (s, SiMe₃).

X-ray Crystallography. Suitable crystals of **3**, **4b**, **5**, and **6a** were obtained by slow diffusion of hexane into a methylene chloride solution of the complexes at room temperature and were mounted on a glass fiber. Crystal data and experimental details are given in Table 1. The data sets for **3**, **4b**, **5**, and **6a**

were collected on an Enraf CAD4 automated diffractometer. Mo Kα radiation (λ = 0.7107 Å) was used for all structures. Each structure was solved by the application of direct methods using the SHELXS-96 program^{27a} and least-squares refinement using SHELXL-97.^{27b} All non-hydrogen atoms in compounds **3**, **4b**, **5**, and **6a** were refined anisotropically. All other hydrogen atoms were included in calculated positions.

Acknowledgment. The support of this research by a Korea Research Foundation Grant (KRF-2000-DPO241) is gratefully acknowledged. This work was also supported by the Brain Korea 21 project in 2000.

Supporting Information Available: Crystallographic data (excluding structure factors) for the structures (**3**, **4b**, **5**, and **6a**) reported in this paper. This material is available free of charge via the Internet at <http://pubs.acs.org>.

OM010892R

(26) Kong, J. W.; Moseley, K.; Maitlis, P. M. *J. Am. Chem. Soc.* **1969**, *91*, 5970.

(27) (a) Sheldrick, G. M. *Acta Crystallogr. A* **1990**, *46*, 467. (b) Sheldrick, G. M. *SHELXL*, Program for Crystal Structure Refinement; University of Göttingen, 1997.